Ecological Engineering 216 (2025) 107621

Contents lists available at ScienceDirect

Ecological Engineering

journal homepage: www.elsevier.com/locate/ecoleng

Mechanisms and benefits of segmented eco-geotechnical measures for debris flow mitigation

Songtang He [a,1], Wenle Chen [a,b,c,1], Xiaoqing Chen [a,*], Daojie Wang [a,*], Yong Li [a], Zengli Pei [a,b], Peng Zhao [a,b], Yuchao Qi [a,b,c,d]

[a] Key Laboratory of Mountain Hazards and Engineering Resilience, Institute of Mountain Hazards and Environment, Chinese Academy of Sciences, Chengdu, China
[b] University of Chinese Academy of Sciences, Beijing, China
[c] Pipe China Southwest Pipeline Company, Chengdu 610095, China
[d] China Petroleum Pipeline Engineering CO., LTD, 065000 Langfang, China

ARTICLE INFO

Keywords:
Debris flow interception
Eco-geotechnical measures
Segmented vegetation filter strip
Comb-toothed dam
Debris flow disaster mitigation

ABSTRACT

Eco-geotechnical measures are increasingly recognized as holistic approaches to disaster mitigation. While the mechanisms underlying disaster mitigation for individual measures (ecological or geotechnical) are relatively well understood, the synergistic benefits and optimal layout of combined models remain unclear. This study proposes an eco-geotechnical model that integrates a segmented vegetation arrangement with comb-toothed dams for debris flow interception. Through field investigations and flume experiment, we delineated the optimal row and stem spacing of segmented vegetation. Additionally, we examined various combination models comprising vegetation filter strips and comb-toothed dams to elucidate their respective benefits and underlying mechanisms in debris flow interception. Results show that optimal interception occurs with tree filter strips at a stem spacing of 6 cm and row spacing of 8 cm and with shrub filter strips at a stem spacing of 3 cm and a row spacing of 4 cm. Moreover, equations were developed for flow velocity reduction and sediment interception, incorporating vegetation layout parameters (e.g., plant spacing, row spacing, number of rows), vegetation morphological parameters (e.g., diameter), and gully bed slope and roughness. Our comparative analysis underscores the superiority of the shrub-grass (dam) model in intercepting dilute debris flows, while the tree-shrub (dam) model excels in mitigating viscous debris flows by achieving notable reductions in flow rate, flow velocity, and sediment interception. Importantly, these findings provide a quantitative basis for optimizing vegetation layouts, advancing nature-based solutions and technologies for comprehensive disaster prevention and mitigation.

1. Introduction

As the influences of climate change and human activities intensify, debris flows often pose severe threats to residential areas, road and bridge infrastructure, river connectivity, and the ecological environment (Marchesini et al., 2024; Riaz et al., 2024). Additionally, a substantial influx of sediment from slopes flanking the main debris flow channel has been observed, serving as a critical source material and further exacerbating the magnitude and destructive impact of debris flow events (Sarkar et al., 2024). Thus, it is particularly important to increase ecosystem resilience and prevent erosion caused by debris flow (Wu et al., 2023). Huang and Zhang (2022) suggest adopting resilience-based approaches that focus on preparing for, responding to, and recovering from unexpected disasters. In this context, nature-based disaster mitigation techniques, especially those pertaining to the role vegetation in disaster prevention and mitigation, have received increasing attention (Anderson and Renaud, 2021; Huai et al., 2021; Kinol et al., 2023), such as modified brush layers and vegetated crib wall (Rey et al., 2019). Nature-based (ecological) solutions are based on natural elements but do not completely rely on nature; therefore, a comprehensive strategy is required. e Ecological measures, like vegetation, and geotechnical measures, like check dams should be combined and used to create a comprehensive disaster mitigation plan based on nature; however, it is more effective than natural solutions (Cui and Lin,

* Corresponding authors.
E-mail addresses: xqchen@imde.ac.cn (X. Chen), wangdj@imde.ac.cn (D. Wang).
[1] Co-first authors.

https://doi.org/10.1016/j.ecoleng.2025.107621
Received 8 November 2024; Received in revised form 2 March 2025; Accepted 26 March 2025
Available online 3 April 2025

2013). The risks posed by natural disasters can be mitigated by utilizing the cooperation between ecological and geotechnical measures (Cui et al., 2021). Geotechnical measures mainly include "blocking, preventing, and draining" measures, such as installing dams for sediment storage, check dams, retaining walls, stock, and diversion troughs. These measurements can effectively prevent and control mountain disasters like debris flows. Ecological measures, such as the arrangement of plants, rely on the mechanical and biological properties of vegetation to regulate the conditions required for disaster formation. For example, forests are strategically planted in water confluence areas, debris flow formation areas, circulation areas, and valley slopes to aid the conservation of water sources, soil, and streambeds, and protect dikes and fluvial fans, respectively.

However, vegetation measures require time and favorable environmental conditions for growth, while geotechnical measures face challenges such as construction difficulties, high costs, and limited-service life. As a result, neither standalone ecological measures nor geotechnical measures can effectively ensure the long-term effectiveness of debris flow prevention and control. At present, the benefits of eco-geotechnical disaster mitigation plans exceed those of plans based on a single measure (ecological or geotechnical), and this phenomenon has been comprehensively documented (Cerrillo et al., 2016). For example, Borja et al. (2018) quantified the effects of check dams and afforestation on sediment mobilization in severely eroded gullies in the Andean Mountains and found that the former measure was highly effective in gullies with active erosion, reducing sediment export by 70 %, whereas the latter had a positive effect on wasteland stabilization and restoration and was effective in reducing sediment transport. Scholars have explained the mechanisms by which such measures contribute to disaster mitigation based on the observed benefits of cooperative eco-geotechnical measures. Among ecological measures, vegetation can improve rainfall interception and reduce surface erosion (Vannoppen et al., 2017; Wahren et al., 2012). Biological processes such as plant transpiration regulate soil physicochemical properties (e.g., pore structure and water content), thus providing additional soil cohesion (Arnone et al., 2016; Chirico et al., 2013), reinforcing loose soil, reducing the source supply of debris flows and underground runoff, and enhancing slope stability (Ng et al., 2017; Stokes et al., 2014; Wang et al., 2020). In addition, trees can also function as rigid structures (Jin et al., 2021) that can withstand the impact of debris flows and rocks and reduce kinetic energy. Tree piles can act as a fence (Guthrie et al., 2010) that inhibits the movement of debris flows, thereby slowing down the mobility of debris (Cui et al., 2023a). Moreover, the spacing between trees can divert debris flows, further inhibiting their movement from material and energy perspectives (Booth et al., 2020). Regarding geotechnical measures, Zou and Chen (2015) investigated the operating status of slot-check dam systems, analyzed and established an evaluation model for intercepting debris flows via windows in slot-check dam systems and proposed a method that allows for analyzing the regulation and self-dredging characteristics of slot-check dams. Their results showed that the arrangement of the slot-check dam system influenced the interception efficacy, with a decreasing trend from upstream to downstream, whereas the influence of the channel slope was relatively small. Based on the properties of substance conservation and, using a comb-toothed dam as the research subject, Sun et al. (2020) investigated the functions of open-check dams in regulating debris flow sediment and movement, particularly discharge process regulation; their work revealed the relationship between regulation and blocking performance. Practical applications of structural innovations in permeable check dams were also undertaken.

Although these studies have improved the optimization of mitigation parameters for ecological and geotechnical measures, research on cooperation between these fields is lacking, and these two measures are still relatively independent. To improve cooperation, Cui and Lin (2013) proposed several integrated plant-geotechnical measures such as terraced fields and contour farming. They found that shortening the slope length and reducing the slope angle through construction or landscape changes increased the time and volume of seepage, thereby reducing soil erosion. Therefore, leveraging the green nature of ecological measures and the immediate effectiveness of geotechnical measures should be fully considered to address the transitional period issue. During this period, the protective strength of geotechnical measures gradually decreases over time, whereas the protective efficiency of ecological measures continues to increase over extended periods. There is a consensus that a combination of ecological and geotechnical engineering can be used to comprehensively control debris flows. However, cooperative eco-geotechnical disaster mitigation models for preventing and controlling debris flows at different scales and frequencies remain rare, and the mechanisms by which these fields cooperate to mitigate disasters remain unclear (Xu et al., 2024). In particular, the mechanism underlying the effects of changes in vegetation row spacing on debris flow interception remains uncertain (He et al., 2023). Therefore, the arrangement of vegetation filter strips must be investigated to optimize debris flow sediment interception in eco-geotechnical measures (i.e., to identify optimal stem and row spacing). This information can provide a reasonable basis for the inclusion of ecological engineering in eco-geotechnical projects. Moreover, cooperation within eco-geotechnical projects with optimal debris-flow control must be explored, as the resulting knowledge will provide a technical basis for establishing eco-geotechnical projects.

Based on the aforementioned issues, to clearly understand the principles and benefits of eco-geotechnical measures in disaster mitigation, this study investigated the integration of ecological engineering and geotechnical engineering to support sediment interception. It established a segmented arrangement model that combines comb-toothed dams and vegetation, and identified key indicators affecting the mitigation benefits of the optimal eco-geotechnical engineering configuration by varying vegetation row and stem spacing in conjunction with comb-toothed dams. Furthermore, the mechanism of disaster mitigation owing to the optimal eco-geotechnical configuration was revealed, and the optimal eco-geotechnical configuration for debris flow interception was identified. The study addresses an existing knowledge gap related to the optimal eco-geotechnical configuration for debris-flow interception and provides a scientific basis and technical support needed to ensure scientific and efficient management of debris flow disasters.

2. Materials and Methods

2.1. Experimental design concept

Field phenomenon showed that vegetation can effectively control the debris flow movement, significantly reducing the movement of debris flows, especially in terms of energy reduction and material interception of large particles (Fig. 1); shrubs can act as interceptors in small-scale debris flows. In slightly larger-scale debris flows, shrubs can increase surface roughness (Fig. 2), which reduces the movement of debris flows. Most importantly, in addition to immediate interception, vegetation substantially changes the local microclimate and enhances system resilience.

Nature-based solutions should be based on natural resources and not restricted to natural measures. The cooperative use of vegetation and geotechnical engineering can address the limitations associated with a single disaster control measure. This study conducted flume experiments to investigate the benefits of using vegetation and geotechnical measures in different spatial combinations for preventing and controlling debris flows. The study observed the effects (flow velocity reduction, flow rate reduction, bulk density, etc.) of changes in tree and shrub row and stem spacing on debris flow prevention and determined the optimal stem and row spacing. Additionally, combinations with comb-toothed dams were evaluated to explore the mechanism underlying the cooperative disaster mitigation model. Finally, the control efficacy of the

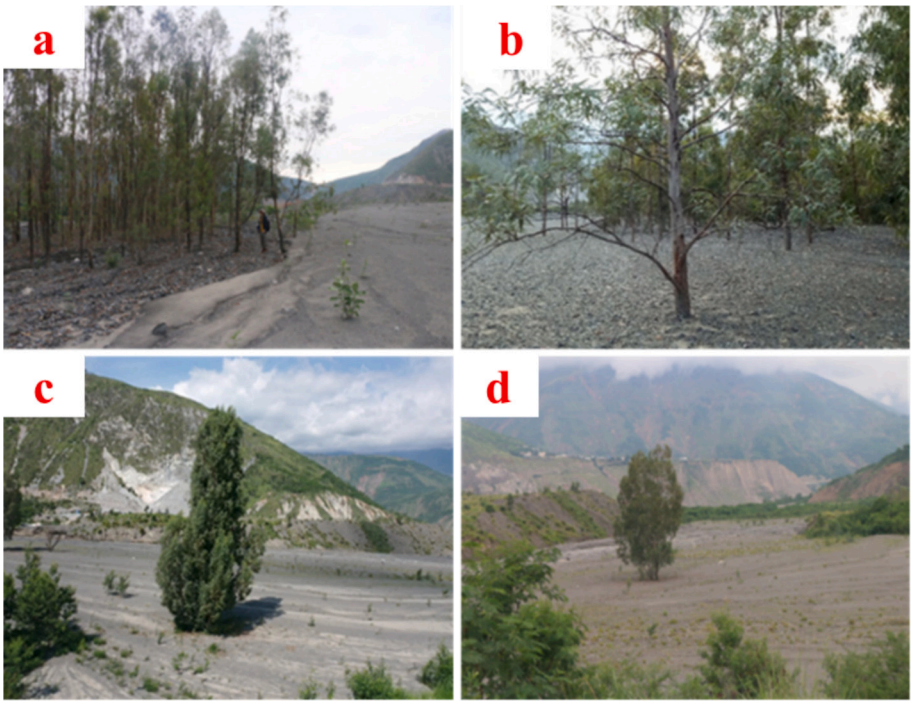

Fig. 1. Examples of the interception ability of trees in preventing debris flows. “a” shows the filtering effect of trees on debris flow, and the coarse particle size is left behind; “b”, “c”, and “d” shows the state of vegetation submerged by debris flow to different degrees, indicating the interception effect of vegetation.

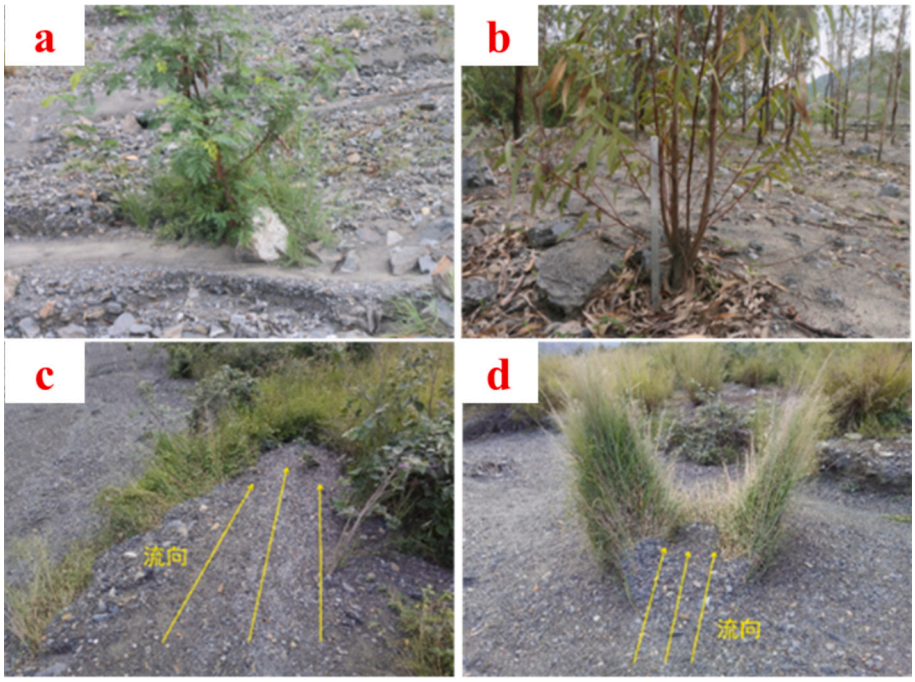

Fig. 2. Examples of the interception abilities of shrubs and grasses in preventing debris flows. “a” and “b” show the blocking effect of branches and stem of shrub on large rocks in debris flow; “c” and “d” demonstrate the dampening effect of herbs on debris flows by increasing surface roughness.

combined methodology was compared with that of a single measure.

Therefore, according to the design concept, the experimental procedure in this study mainly included three steps. (1) A standalone tree-intercepting debris flow experiment was conducted, and the levels of interception under different row and stem spacings were compared to determine the optimal row and stem spacings. (2) A standalone shrub-intercepting debris flow experiment was conducted, and the interception benefits under different row and stem spacings were compared to determine the optimal row and stem spacings. (3) The optimal tree and shrub row and stem spacings obtained in (1) and (2) were combined with comb-toothed dams and arranged in segments in a simulated gully to explore the cooperative disaster mitigation benefits of these approaches (Fig. 3). The arrangement of the comb-toothed dams was based on Sun et al. (2020).

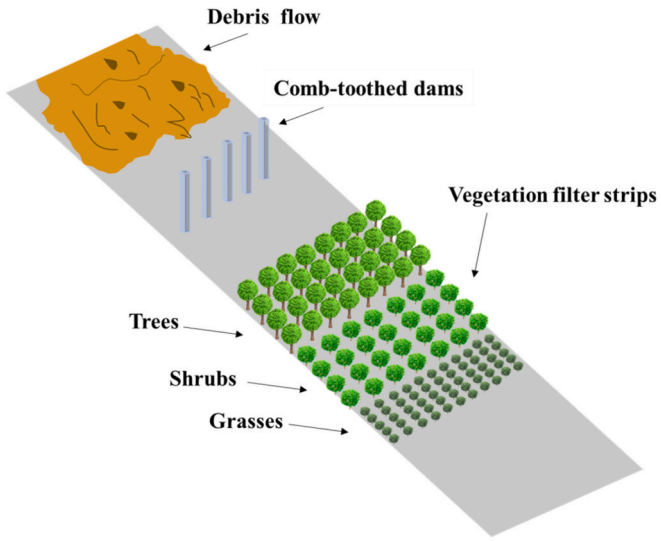

Fig. 3. Experimental design diagram of the cooperative model integrating segmented vegetation types and pile-forest dams.

Table 1
Morphological characteristics of *Leucaena leucocephala*.

Tree species	Quantity (plants)	Plant height (m)	Crown width (m)	Diameter at breast height (m)
Leucaena leucocephala	67	10.23 + 1.256	4.8 × 5.6	0.15 + 0.876

2.2. Vegetation parameter survey and scale description

The Jiangjiagou area, which is a typical debris-flow outbreak region (http://nsl.imde.ac.cn/en/), was selected as the study area. The composition and movement characteristics of dilute and viscous debris flows have been investigated through in-situ observations and modelling experiments (Song et al., 2021, 2023). In the present study, eco-geotechnical measures were applied to varying degrees to represent typical applications. The morphological characteristics of the trees, shrubs, and grasses were investigated using quadrat surveys. The dimensions of the quadrats were 20 × 20 m. The diameter at breast height, plant height, and crown width of the pioneer tree species *Leucaena leucocephala* were measured, as shown in Table 1. The spacing between trees was 5–10 m.

The survey revealed that the aboveground parts of L. *leucocephala* in the quadrats could be divided into two sections. The first section included an upright trunk under a canopy. This section of the trunk was relatively straight, with a uniform diameter from top to bottom and without any branches. Measurements revealed that the length of the unbranched trunk section under the canopy was approximately 4–6 m (Fig. 4), and the second section included the canopy with numerous branches. Based on the measurements shown in Table 1 and the length scale of the test (1:50), the height of the tree models used in the test was 20 cm, and the diameter at breast height was 0.6 cm (Fig. 5).

The shrubs in the Jiangjiagou watershed are dominated by *Coriaria sinica*, which grows in tributaries and has useful soil and water conservation properties. *C. sinica* is also a pioneer species in terms of vegetation recovery following collapses and landslides, and is effective in suppressing gravity erosion in debris flow areas. *C. sinica* is tolerant of low-nutrient environments and has a strong adaptability, rapid growth, and high erosion resistance. As an ideal plant for the bioengineering-based control of debris flows, *C. sinica* has been extensively planted in dry and hot valleys. The shrub survey was conducted in quadrats measuring 5 m × 5 m (Fig. 6). Surface morphological characteristics such as the base diameter, number of base branches, plant height, and crown width were recorded. The survey results are summarized in Table 2.

Based on the results of the field survey and a test scale of 1:50, the height of the shrub models was 4.5 cm, and the number of basal branches was six (Table 2).

The herbaceous vegetation distributed in the Jiangjiagou Watershed was dominated by *Heteropogon contortus* (Fig. 7), and the size of the quadrat was set to 5 m × 5 m. Surface morphological characteristics such as plant height, base diameter, and crown width were surveyed. The results are summarized in Table 3.

This survey showed that *H. contortus* is tolerant to drought and low-nutrient environments, grows rapidly, and can rapidly grow and reproduce in nutrient-poor debris flow valleys. *H. contortus* has a

Fig. 4. Quadrat survey of *Leucaena leucocephala* (a and b) and aboveground part of *Leucaena leucocephala* (c and d).

Fig. 5. Tree models used in the flume experiment, and a single tree parameter: height is 20 cm, and the diameter is 0.6 cm.

clustered morphology. The stalks of the plants are upright and sparse at the top and dense at the bottom, and the diameter of the base is approximately 0.45 m; thus, the sediment interception range is wide. In addition, the stalks of *H. contortus* are rigid and have a strong resistance, and the root system of *H. contortus* is thoroughly developed; thus, *H. contortus* has a strong sediment interception ability. Based on the results of the field investigation at a scale of 1:50, the height of the herbaceous plant model was 3 cm.

2.3. Flume experiment procedures

2.3.1. Tree filter strip test

In the tree filter strip experiment, the stem and row spacing of the tree strips were modified to investigate their ability to filter debris. The stem spacing was set to 6, 8, 10, and 12 cm in the test, at a scale of 50:1, the corresponding actual stem spacings were 3, 4, 5, and 6 m, respectively. The row spacings in the test were set to 8, 10, 12, 14, and 16 cm, and at a scale of 50:1, the corresponding actual row spacings were 4, 5, 6, 7, and 8 m. The number of tree rows in each group was 7; according to previous studies (Zhao et al., 2016), the staggered arrangement of plants in a zigzag pattern more strongly improved water and sand retention than a parallel arrangement, so the vegetation in this study was arranged in a zigzag pattern (Fig. 8). When studying the effect of stem spacing on the regulation of debris flows, only stem spacing was changed, whereas row spacing remained unchanged at 16 cm. When studying the effect of row spacing on the regulation of debris flows, only row spacing changed, whereas the stem spacing remained unchanged at 6 cm. Eighteen groups of tree filter strip tests were established, including 16 groups of tree filter strip tests with different arrangement parameters and two groups of control tests. The test settings for the 16 groups with different arrangement parameters are listed in Table 4. The three filter strips were arranged downstream beginning at 2.5 m from the top of the flume (Fig. 8). The range was determined by the length of the filter strip, which varied with row spacing.

2.3.2. Shrub filter strip test

In the shrub filter strip experiment, the stem and row spacing were altered to investigate the regulatory effects of shrub filter strips on debris flows. The stem spacing was set to 3, 4, 5, and 6 cm in the experiments; at a scale of 50:1, the corresponding actual stem spacings were 1.5, 2, 2.5, and 3 m, respectively. The row spacings were set to 4, 6, 8, 10, and 12 cm, and at a scale of 50:1, the corresponding actual row spacings were 2, 3, 4, 5, and 6 m, respectively. Each group consisted of shrub rows in each group was 7. Similar to the tree filter strip, shrub vegetation was staggered in a zigzag pattern. When studying the effect of stem spacing on the regulation of debris flows, only stem spacing was changed, whereas row spacing remained unchanged at 12 cm. When studying the effect of row spacing on the regulation of debris flows, only row spacing changed, whereas stem spacing remained unchanged at 3 cm. Sixteen groups were established for the shrub filter strip test (Table 5). Shrub filter strips were also arranged 2.5 m downstream of the top of the flume (Fig. 9). The arrangement range was determined by the length of the filter strips, which varied with row spacing.

Table 2
Morphological characteristic parameters of Coriaria sinica.

Tree species	Quantity (plants)	Plant height (m)	Crown width (m)	Base diameter (cm)	Number of basal branches
C. sinica	25	2.23 + 0.652	2.1 × 2.2	15	6

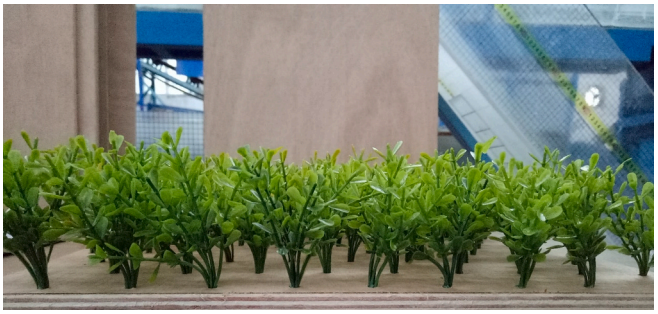

Fig. 7. Shrub models used in the flume experiment.

Table 3
Morphological characteristics of *Heteropogon contortus*.

Species	Quantity (plants)	Plant height (m)	Crown width (m)	Base diameter (m)
H. contortus	20	1.68 + 1.012	1.2 × 1.1	0.45

2.3.3. Eco-geotechnical cooperative sediment interception experimental protocol

The optimal row and stem spacing for trees and shrubs were obtained

Fig. 6. Quadrat survey of *Coriaria sinica* within the scope of 5 m × 5 m, and measure and record the base diameter, number of base branches, plant height, and crown width.

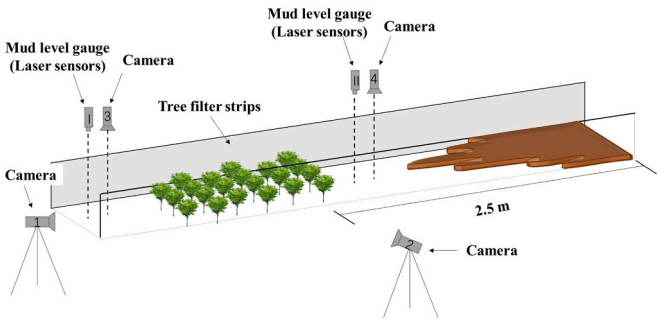

Fig. 8. Layout of the tree filter strips in the flume experiment. Cameras are used to record the process of debris flow movement; mud level gauges are used to record the tracks of debris flow when it goes through different measures.

(see Sections 2.1 and 2.2), and the disaster mitigation benefits under different models were further studied by comparing different combinations of trees, shrubs, and dams. It is worthy of being pointed out there are two design principles: one is the spacing can allow vegetation to grow in an unrestricted space; the other is vegetation can effectively control debris flow movement. Meanwhile, debris flow, passed through the dams to vegetation filter strip, are weaken. According to the field investigation, the spacing range finally was determined. The ecological model included seven different combinations, namely tree-shrub-grass, tree-shrub, tree-grass, shrub-grass, tree, shrub, and grass; seven combinations of comb-toothed dams were also utilized, namely dam-tree-shrub-grass, dam-tree-shrub, dam-tree-grass, dam-shrub-grass, dam-tree, dam-shrub, and dam-grass. According to existing knowledge on energy reduction and material interception, the impact force of debris flows subjected to upstream control measures is greater than that of debris flows subjected to downstream control measures. Therefore, upstream measures should have a greater stiffness than downstream measures to withstand the impact of debris flows, thus reducing debris flow intensity. Therefore, the comb-toothed dam was arranged 1.5 m from the top of the flume, and vegetation filter strips were arranged 2 m from the top of the flume, with a fixed length of 1.5 m (Fig. 10).

2.4. Experimental setup and equipment

We conducted experiments at the Dongchuan Debris Flow Observation and Research Station (DDFORS) of the Chinese Academy of Sciences. As shown in Fig. 11, the test equipment included a hopper (0.6 m × 0.6 m × 0.7 m), a generalized flume (4 m × 0.4 m × 0.4 m, longitudinal gradient: 0–15°), a comb-toothed dam (width: 0.4 m, height: 0.2 m, comb tooth spacing: 2.5 cm, comb tooth width: 2 cm), tree models (height: 20 cm, diameter at breast height: 0.5 cm), shrub models (height: 5 cm, base diameter: 0.3 cm, basal branches: 6), herb models (height: 3 cm), black plastic bottom plates, and buckets for collecting tailings. The ratio of the tree, shrub, herb, and comb-toothed dam models was 1:50.

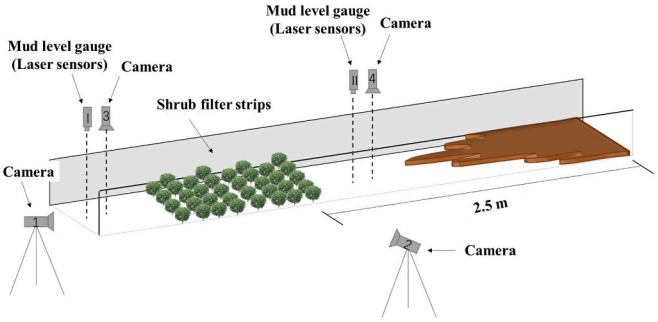

Fig. 9. Layout of shrub filter strips in the flume experiment. Cameras are used to record the process of debris flow movement; mud level gauges are used to record the tracks of debris flow when it goes through different measures.

Table 4
Layout parameters of the tree filter strips used in the flume experiment.

No.	1	2	3	4	5	6	7	8
Stem spacing (cm)	6	6	8	8	10	10	12	12
Row spacing (cm)	16	16	16	16	16	16	16	16
Number of rows	7	7	7	7	7	7	7	7
Bulk density (t/m^3)	1.5	2.0	1.5	2.0	1.5	2.0	1.5	2.0
Planting density (plants/m^2)	0.042	0.042	0.031	0.031	0.025	0.025	0.021	0.021
Tree filter length (m)	0.96	0.96	0.96	0.96	0.96	0.96	0.96	0.96
No.	9	10	11	12	13	14	15	16
Stem spacing (cm)	6	6	6	6	6	6	6	6
Row spacing (cm)	8	8	10	10	12	12	14	14
Number of rows	7	7	7	7	7	7	7	7
Bulk density (t/m^3)	1.5	2.0	1.5	2.0	1.5	2.0	1.5	2.0
Planting density (plants/m^2)	0.083	0.083	0.067	0.067	0.056	0.056	0.048	0.048
Tree filter length (m)	0.48	0.48	0.6	0.6	0.72	0.72	0.84	0.84

Table 5
Layout parameters of shrub filter strips in the flume experiment.

No.	1	2	3	4	5	6	7	8
Stem spacing (cm)	3	3	4	4	5	5	6	6
Row spacing (cm)	12	12	12	12	12	12	12	12
Number of rows	7	7	7	7	7	7	7	7
Bulk density (t/m^3)	1.5	2.0	1.5	2.0	1.5	2.0	1.5	2.0
Planting density (plants/m^2)	0.111	0.111	0.083	0.083	0.067	0.067	0.056	0.056
shrub filter length (m)	0.72	0.72	0.72	0.72	0.72	0.72	0.72	0.72
No.	9	10	11	12	13	14	15	16
Stem spacing (cm)	3	3	3	3	3	3	3	3
Row spacing (cm)	4	4	6	6	8	8	10	10
Number of rows	7	7	7	7	7	7	7	7
Bulk density (t/m^3)	1.5	2.0	1.5	2.0	1.5	2.0	1.5	2.0
Planting density (plants/m^2)	0.333	0.333	0.222	0.222	0.167	0.167	0.133	0.133
Shrub filter length (m)	0.24	0.24	0.36	0.36	0.48	0.48	0.6	0.6

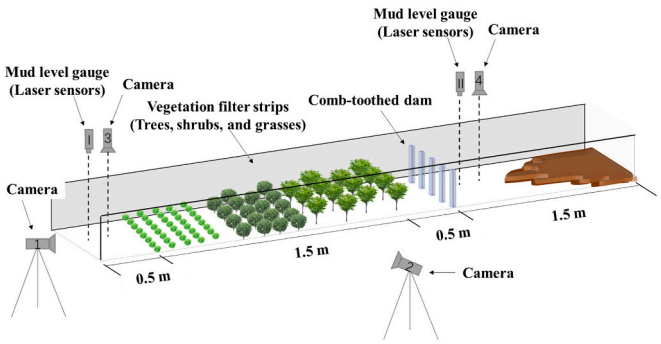

Fig. 10. Layout of eco-geotechnical engineering in the flume experiment. The order of placement of measures are Comb-tooted dam, trees, shrubs, and grass. Cameras are used to record the process of debris flow movement; mud level gauges are used to record the tracks of debris flow when it goes through different measures.

During the test, Sony HDR-CX610E cameras were set up on the front, side, and top of the flume to record the entire test process, and a mud-level gauge was set up downstream of the flume to record changes in the mud level resulting from the debris flow.

We maintained geometric similarity with a contraction ratio of $n = 50$ (where n represents the ratio of the actual geometric size to the experimental size), ensuring consistency in length scale. To characterize the balance between inertial and gravitational forces in the flowing materials, we employed the dimensionless Froude number (Fr), thereby establishing dynamically similar conditions to real-world debris flows. According to previous studies (Heller, 2011; Lobovský et al., 2014), the Fr values of natural debris flows are generally below 5.0. In this study, the incoming debris flow exhibited Fr values ranging from 2.5 to 3.2, which falls within the typical range observed in field events (Kwan et al., 2015; Mcardell et al., 2007). This suggests that the experimental conditions are representative of natural debris flow dynamics.2.5 Data acquisition and calculation at the end of each group of tests, the relevant data were measured, and some data were obtained through a later interpretation of the test videos.

2.5. Data acquisition and calculation

At the end of each group of tests, the relevant data were measured, and some data were obtained through a later interpretation of the test videos. The measured parameters and methods used in this experiment are detailed in the following sections.

2.5.1. Bulk density and volume of debris flow tailings

The experimental material is the reconstructed debris flow, consisting of debris flow deposits from the Jiangjiagou Gully that passed through a 2 cm sieve, and then were mixed with water to form viscous and dilute debris flows with bulk densities of 2.0 and 1.5 g/cm^3 (Tables 4, 5, & 6), respectively. It is worthy of being pointed out viscous debris flows are characterized by a high clay content, with solid materials comprising 40–60 %—and in some cases up to 80 %—resulting in a bulk density exceeding 1.8 g/cm^3. In contrast, dilute debris flows consist primarily of water with only a small proportion of clay, where solid materials make up 10–40 %. These flows exhibit significant dispersion and have a lower bulk density, ranging from 1.5 to 1.8 g/cm^3 (Pudasaini and Mergili, 2019; Tjalling et al., 2015). At the end of the experiment, the debris flow tailings in the collection bucket were weighed and expressed as m_1, and the bucket mass was recorded as m_2. A steel ruler was used to measure the mud depth (H) of the debris flow in the bucket, and the volume (V) of the debris flow in the bucket was calculated based on the relationship between the mud depth and volume of liquid in the bucket. Then, the specific weight of the debris flow tailings was calculated as follows:

$$\rho = \frac{m_1 - m_2}{V}\# \tag{1}$$

2.5.2. Mud depth H of the debris flow

The mud depths (H) before and after the filter strips were directly measured using a laser mud-level gauge installed above the flume.

2.5.3. Debris flow velocity

A camera was used to capture images of the debris-flow process, and through subsequent video interpretation, the travel distance (s) of a buoy over time (t) was obtained using the conventional buoy measurement method. The debris-flow velocity (v) was obtained using Eq. (3.2).

$$v = \frac{s}{t}\# \tag{2}$$

2.5.4. Flow rate Q

Based on the interpreted debris flow velocity (v) and mud depth (h) measured by the mud-level gauge, the flow rate was calculated by Eq. (3.3).

$$Q = 0.4 \times v \times h\# \tag{3}$$

where 0.4 is the width of the flume (m).

2.5.5. Amount of sediment retention m_{sr} and sediment retention rate P_s

At the end of the test, the debris flow tailings were collected, air-dried, and weighed to obtain the weight of the sediment being flushed

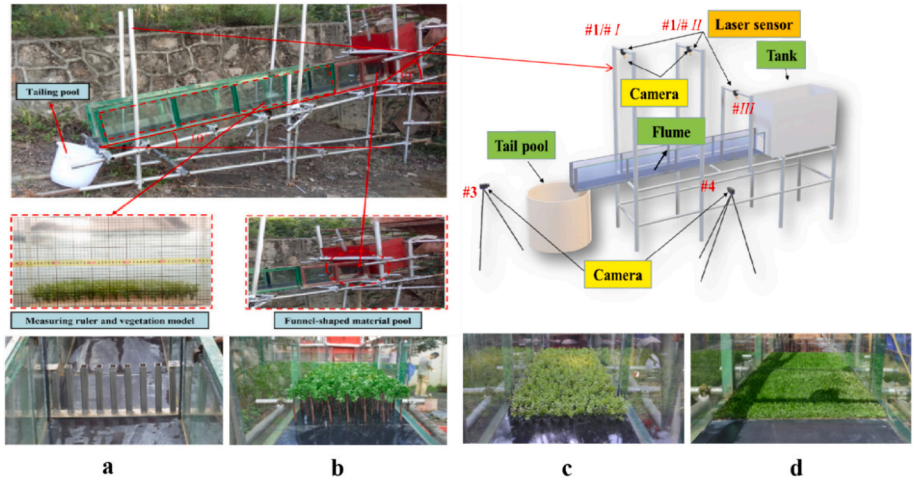

Fig. 11. Experimental layout and measuring instrument installation diagram. a: comb-toothed dam, b: trees, c: shrubs, d: grasses.

Table 6
Parameters of eco-geotechnical engineering test.

No.	1	2	3	4	5	6	7	8
Pattern	Tree-shrub-grass	Tree-shrub-grass	Tree-shrub-grass-dam	Tree-shrub-grass-dam	Tree-shrub	Tree-shrub	Tree-shrub-dam	Tree-shrub-dam
Bulk density	1.5	2.0	1.5	2.0	1.5	2.0	1.5	2.0
No.	9	10	11	12	13	14	15	16
Pattern	Tree-grass	Tree-grass	Tree-grass-dam	Tree-grass-dam	Shrub-grass	Shrub-grass	Shrub-grass-dam	Shrub-grass-dam
Bulk density	1.5	2.0	1.5	2.0	1.5	2.0	1.5	2.0
No.	17	18	19	20	21	22	23	24
Pattern	Tree	Tree	Tree-dam	Tree-dam	Shrub	Shrub	Shrub-dam	Shrub dam
Bulk density	1.5	2.0	1.5	2.0	1.5	2.0	1.5	2.0
No.	25	26	27	28	29	30	31	32
Pattern	Grass	Grass	Grass-dam	Grass-dam	Dam	Dam	None of measures (control group)	None of measures (control group)
Bulk density	1.5	2.0	1.5	2.0	1.5	2.0	1.5	2.0
No.	1	2	3	4	5	6	7	8
Pattern	Tree-shrub-grass	Tree-shrub-grass	Tree-shrub-grass-dam	Tree-shrub-grass-dam	Tree-shrub	Tree-shrub	Tree-shrub-dam	Tree-shrub-dam

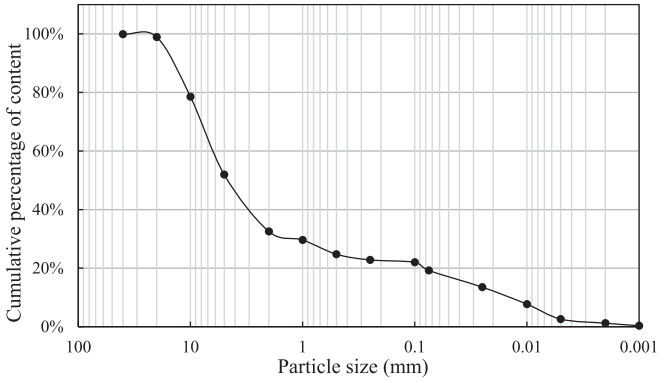

Fig. 12. Grading curve of original materials obtained by Malvern (United Kingdom) MS2000 laser particle size analyzer (He et al., 2023).

out, m_{so}. The weight of the sediment flowing into the tank is m_{si}; thus, the sand retention amount was calculated as follows:

$$m_{sr} = m_{si} - m_{so}\# \tag{4}$$

The sand retention rate was determined as follows:

$$P_s = 1 - \frac{m_{so}}{m_{si}}\# \tag{5}$$

2.5.6. Particle size characteristics of flushed debris flow sediments

A vibrating sieve and laser particle size analyzer were used to conduct a particle size test, and a particle size grading curve was plotted to obtain the particle size characteristics of the debris flow samples. The vibrating sieve was mainly used to test the particle size distribution of the particles larger than 0.25 mm in the sample. The sieves were 20, 10, 5, 2, 1, 0.5, and 0.25 mm in size; the shaking time was set to approximately 10 min, and weighing was performed after the shaking stopped. The particles that were smaller than 0.25 mm and remained in the sieve tray were measured using a Malvern (United Kingdom) MS2000 laser particle size analyzer (Fig. 12).

2.6. Derivation of flow velocity reduction formulas for the tree and shrub filter strips

The flow velocity reduction formula for a shrub filter strip was first

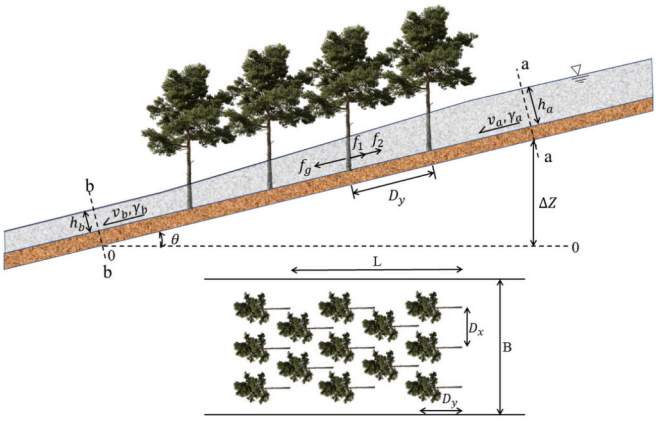

Fig. 13. Process by which a tree filter strip blocks a debris flow. The stem spacing is D_x, the row spacing is D_y, the number of rows is N, and the length of the filter strip is $L = (n\text{-}1)^* D_y$. The width of the gully channel is B. Due to the staggered planting of trees in the filter strip, the number of trees in each row is $[B/ D_x]$ (rounded) or $[B/ D_x] + 1$, and the slope of the gully bed is θ.

derived by He et al. (2023), and this formula was utilized for a tree filter strip in the present study. Based on the test data obtained, the flow velocity reduction formula for a tree filter strip that considered influencing factors such as vegetation surface morphological characteristics, vegetation filter strip arrangement parameters (stem spacing, row spacing, and number of rows), and debris properties (specific weight, flow velocity, and mud depth) was established.

Fig. 13 shows a schematic diagram of the process by which a tree filter strip blocks a debris flow. The 0–0 horizontal plane was used as the datum. The upstream cross-section a-a and downstream cross section b-b of the three filter strips were taken. 1) Before the filter strip, the flow velocity is v_a, the elevation is z_a, the mud depth is h_a, the specific weight is γ_a, and the pressure is p_a; 2) after the filter strip, the flow velocity is v_b, the elevation is z_b, the mud depth is h_b, the specific weight is γ_b, and the pressure is p_b.

The debris flow is assumed to be a constant fluid; that is, time is used as the standard and the flow parameters (velocity, pressure, density, etc.) at spatial points do not vary with time. The vertical and lateral distributions of the flow velocity were not considered, and h_f represents the head or energy loss of the debris flow. Based on the Bernoulli

equation, the following equations were obtained:

$$v_b = \sqrt{v_a^2 + 2g\left[L\sin\theta - \frac{\lambda v^2 L \times (vB^2 + Q)}{4QBg}\right]}\# \quad (6)$$

$$L = (N-1)D_y\# \quad (7)$$

$$\lambda = \frac{1}{(1-f_v)}\left[\frac{8n_0^2 g}{R^2} + \frac{4C_D\sum_{i=k}^{N} A_i}{\chi^2}\right]\# \quad (8)$$

$$f_v = \frac{\sum_{i=1}^{M} T_{vi}}{AL}\# \quad (9)$$

$$R = \frac{A}{\chi} = \frac{(B-md)h}{2h(m+1)+B-md}\# \quad (10)$$

$$m = \left[\frac{B}{D_x}\right] + 1\# \quad (11)$$

$$M = N\left[\frac{B}{D_x}\right] + \frac{N}{2}\# \quad (12)$$

N is an even number, and B/D_x is not an integer.

$$M = N\left(\left[\frac{B}{D_x}\right] - 1\right) + \frac{N}{2}\# \quad (13)$$

N is an even number, and B/D_x is an integer.

$$M = N\left[\frac{B}{D_x}\right] + \frac{N+1}{2}\# \quad (14)$$

N is an odd number, and $B/D_x$is not an integer.

$$M = N\left(\left[\frac{B}{D_x}\right] - 1\right) + \frac{N+1}{2}\# \quad (15)$$

N is an odd number, and$B/D_x$is not an integer.

where: v_a is the flow velocity before the filter strip, v_b is the flow velocity after the filter strip, D_x is the stem spacing, D_y is the row spacing, N is the number of rows, L is the length of the filter strip, B is the width of the valley, θ is the slope of the gully bed, λ is the friction coefficient, v is the average flow velocity ($v = (v_a + v_b)/2$), Q is the flow rate, f_v is the submerged volume ratio of the tree filter strip in the debris flow, n_0 is the Manning roughness coefficient of the nonfiltered zone (i.e., the original gully bed roughness), R is the hydraulic radius, C_D is the flow resistance coefficient around the vegetation, which is generally related to the shape of the vegetation and the Reynolds number of the debris flow R_e, A_i is the projected area of a row of trees on the cross-section orthogonal to the flow direction, χ is the wetted perimeter, A is the flow area, T_{vi} is the submerged volume of each tree in the debris flow and is related to the plant species and surface morphological characteristics, M is the total number of plants in the filter strip, m is the number of trees in each row, d is the diameter of the trunks of the trees, and h is the depth to which the trees were submerged in mud.

3. Results

3.1. Optimal tree-shrub arrangement parameters

Fig. 14 and Fig. 15 show the effects of different stem and row spacing combinations for trees and shrubs on debris flow reduction. For different stem and row spacing combinations of trees, the sediment interception rate, flow-velocity reduction rate, flow-rate reduction rate, and bulk-density reduction rate of dilute debris flow were 12.20–26.20 %, 6.70–26.20 %, 0.49–15.04 %, 2.30–7.20 %, respectively. The sediment interception rate, flow-velocity reduction rate, flow-rate reduction rate, and bulk-density reduction rate of viscous debris flow were 39.70–62.20 %, 11.30–39.90 %, 4.59–34.18 %, and 0.10–3.20 %, respectively. Comparisons revealed that a stem spacing of 6 cm and row spacing of 8 cm facilitated the greatest reductions.

For different stem and row spacing combinations of shrubs, the sediment interception rate, flow-velocity reduction rate, flow-rate reduction rate, and bulk-density reduction rate of dilute debris flow were 27.40–70.70 %, 18.00–44.90 %, 18.52–46.83 %, and 8.00–27.60 %, respectively. The sediment interception rate, flow-velocity reduction rate, flow-rate reduction rate, and bulk-density reduction rate of dilute debris flow of viscous debris flow were 39.00–66.30 %, 15.70–34.20 %, 23.29–47.35 %, and 0.50–5.30 %, respectively. Comparisons revealed that the combination of a stem spacing of 3 cm and row spacing of 4 cm facilitated the greatest reductions. The optimal stem and row spacing of trees and shrubs were used as vegetation arrangement parameters for subsequent eco-geotechnical cooperative disaster mitigation tests, and the debris flow-interception rate captured using vegetation and comb-toothed dams was further investigated.

3.2. Reduction effects on dilute debris flows

Fig. 16 shows the reduction intensities of different combined models on the movement of dilute debris flows. Overall, the disaster mitigation indicators of flow velocity reduction, flow rate reduction, and sediment interception were most marked. However, the reduction in each indicator varied among the combined models. Under the vegetation models, the reduction rates on the debris flow velocity (referring to the difference in flow velocity before and after the vegetation filter strip) from large to small were as follows: shrub-grass (69.21 %), tree-shrub (61.52 %), grass (56.94 %), shrub (51.53 %), tree-grass (43.11 %), tree-shrub (38.52 %), and trees (13.11 %). The addition of the comb-toothed dam did not alter the flow velocity reduction observed for the vegetation models, but the reduction rate following the addition of the comb-toothed dam increased to varying degrees compared with that under the vegetation models, in the following order: shrub-grass-dam (70.81 %), tree-shrub-dam (67.72 %), grass-dam (59.22 %), shrub-dam (53.76 %), tree-grass-dam (45.44 %), tree-shrub-dam (41.51 %), and tree-dam (15.42 %).

The ranking of the vegetation models from highest to lowest in terms of debris flow rate reduction was the same as that of the flow rate reduction. Except for the tree model (with a reduction rate of only 8.13 %), the other combined models exhibited relatively high flow rate reduction rates, with that of the shrub-grass model reaching 71.04 %. When combined with a comb-toothed dam, the flow rate reduction rate increased to varying degrees, with that of the shrub-grass-dam model being the highest at 74.21 %, and that of the tree-dam model approaching 10 %.

Among the vegetation models, sediment interception was highest for the shrub-grass model (74.83 %) and lowest for the tree model (24.91 %). When combined with a comb-toothed dam, the interception rates increased to varying degrees, with that of the shrub-grass-dam model being the highest (77.64 %) and that of the tree-dam model being the lowest (35.62 %). Although the sediment retention rates of the combined models mostly followed the same ranking as that of the flow velocity and flow rate reductions, the efficacy of the tree-shrub (dam) model was superior to that of the tree-grass (dam) model.

Although both the vegetation and cooperative models (those that combined vegetation and comb-toothed dams) had considerable effects on the velocity, flow rate, and sediment interception, the reduction in the specific weight of the dilute debris flow was not substantial. Among the vegetation models, the shrub-grass model exhibited the strongest reduction (26.33 %), whereas the tree model exhibited the weakest reduction (4.14 %). The incorporation of comb-toothed dams led to increased efficacies, with the reduction rate of the shrub-grass-dam model increasing to 27.42 % and that of the tree-dam model increasing to 8.58 %.

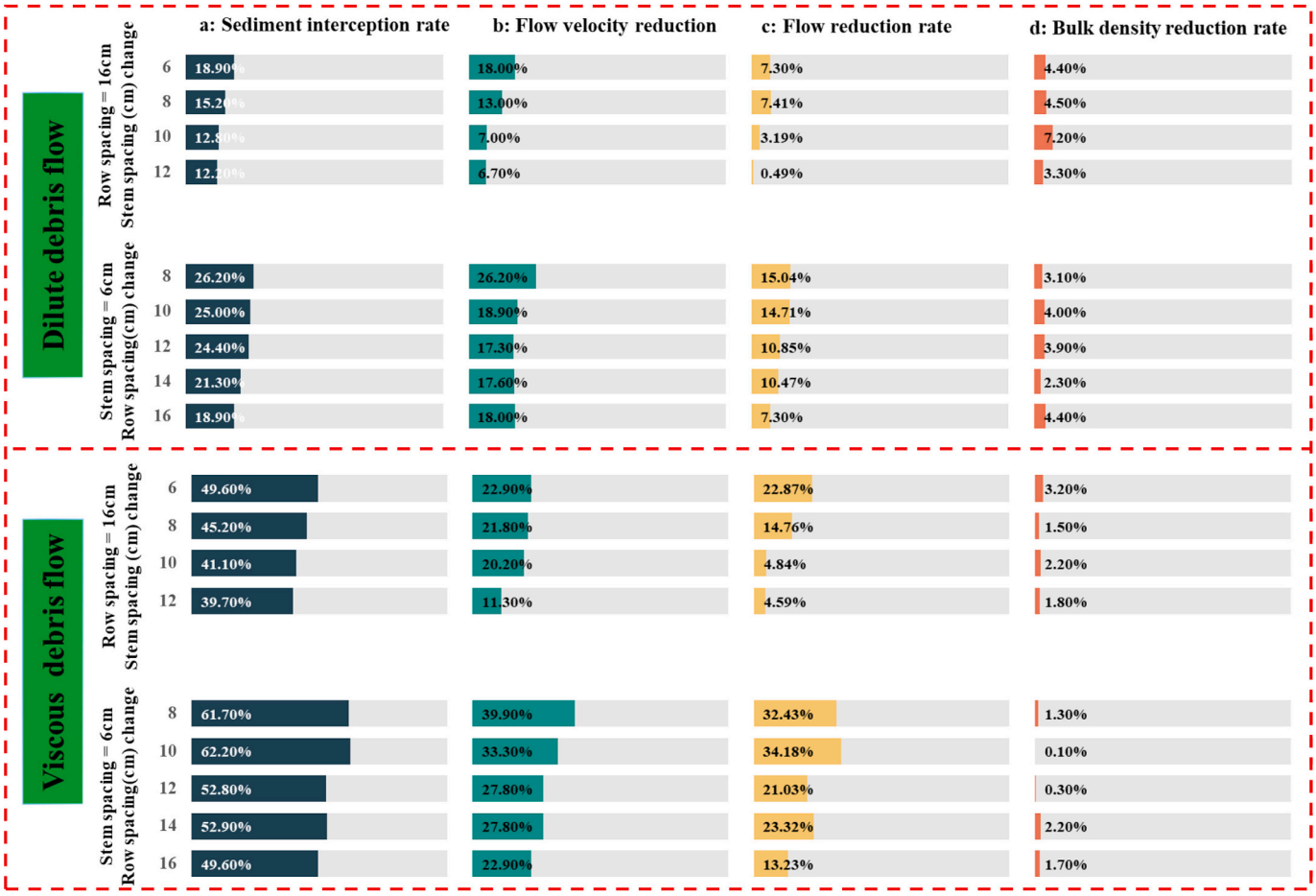

Fig. 14. Reduction efficacies of different stem and row spacing combinations of trees on dilute debris flows. a: sediment interception, b: flow velocity interception, c: flow rate reduction, and d: bulk density reduction.

3.3. Reduction effects on viscous debris flows

Fig. 17 shows the reduction rates of the different models with different combinations of approaches for the movement of viscous debris flows. Overall, the reduction rate of the vegetation-geotechnical cooperative models on debris flows was greater than that of the vegetation models, and the reductions in flow velocity, flow rate, and sediment interception were marked; however, there were differences among the models. Among the vegetation models, the tree-shrub model had the greatest reduction on flow velocity (48.92 %), whereas the grass model had the smallest reduction (8.71 %). However, after integrating the comb-toothed dams, the reduction rate of the tree-shrub-dam model was the highest (65.23 %) and the reduction rate of the grass dam was the lowest (31.54 %). The reduction in flow velocity was significantly greater in the eco-geotechnical measures, and the reduction intensity of the grass-dam model increased by 2.62 times.

Among the vegetation models, the tree-shrub model had the greatest reduction (64.82 %) on viscous debris flow rates, and the grass model had the weakest reduction at 16.01 %. The effects of the combination models in terms of reduction were as follows: tree-shrub > tree-shrub-grass > tree-grass > tree > shrub > shrub-grass > grass. However, after integrating the comb-toothed dams into the models, the flow rate decreased by varying degrees. The tree-shrub-dam model had the greatest flow rate reduction (81.82 %), and the disaster mitigation rate increased by 26.23 % compared to that of the pure vegetation model. The grass-dam model had the smallest reduction rate (37.03 %), and the disaster mitigation rate increased by 131.29 %.

In the vegetation models, sediment interception was ranked as follows (in descending order): tree-shrub > tree-shrub-grass > shrub > shrub-grass > tree-grass > grass > trees. The maximum and minimum interception rate were 68.83 and 28.87 %, respectively. After integrating the comb-toothed dams, the maximum interception rate of the tree-shrub-dam model reached 92.41 %, which comprised an increase of 34.26 %, and the tree-dam model had the lowest interception rate of 37.52 %.

4. Discussion

4.1. Validation of the formula for flow velocity reduction after traversing the tree filter strip

The flow velocity reduction equation for the tree filter strip is as follows:

$$P = 1 - \frac{v_b}{v_a}\# \tag{16}$$

Substituting Eqs. (6) into (16) gives the following.

The flow velocity reduction equation for a dilute debris flow is as follows:

$$P_v = 1 - 1.5078\sqrt{1 + \frac{2Q}{v_a^2}\left[Lsin\theta - \frac{\lambda v^2 L \times (vB^2 + Q)}{4QBg}\right]} + \frac{0.3699}{v_a}\# \tag{17}$$

The flow velocity reduction equation for a viscous debris flow is as follows:

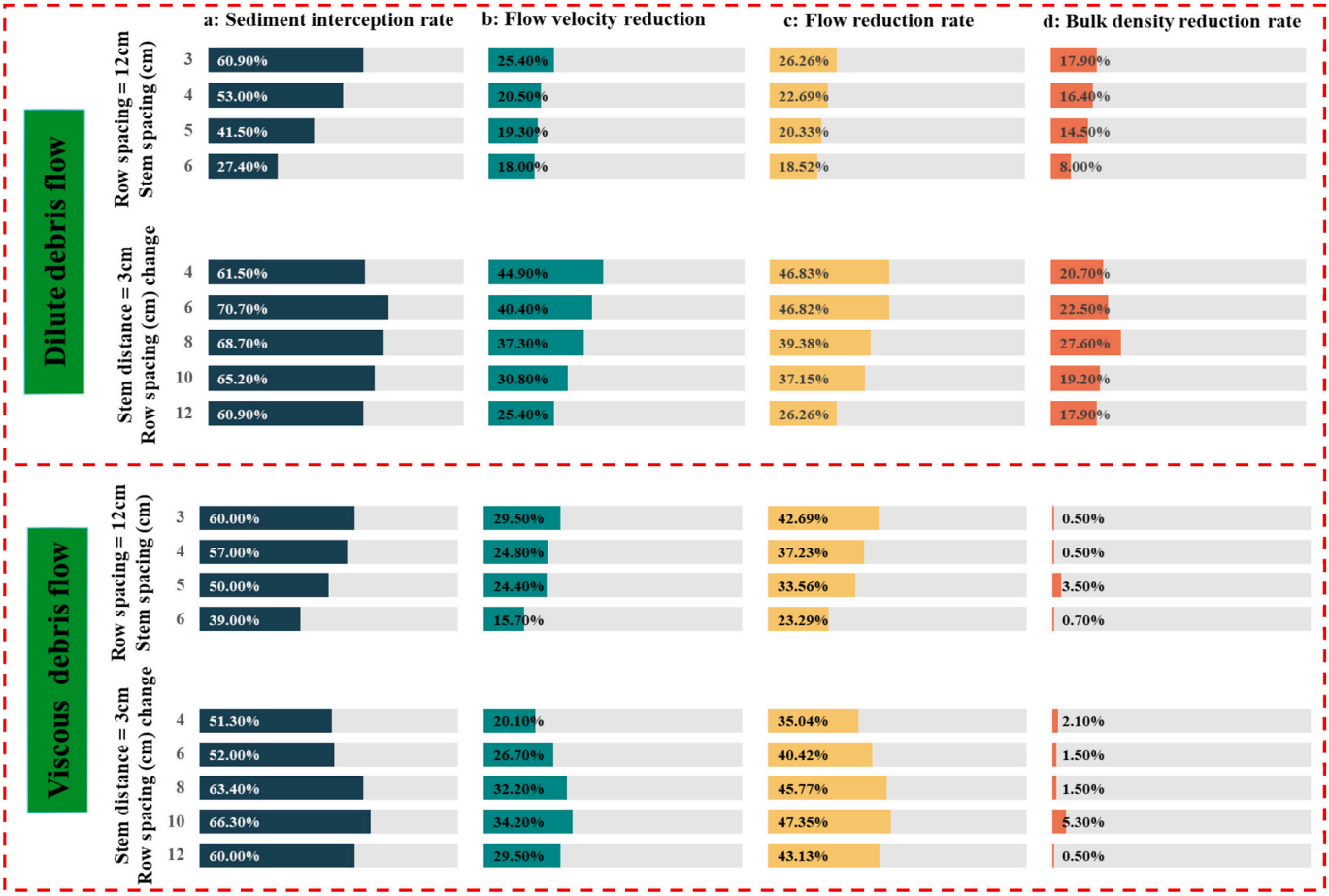

Fig. 15. Reduction efficacies of different stem and row spacing combinations of shrubs on viscous debris flow movement. a: sediment interception, b: flow velocity interception, c: flow rate reduction, and d: bulk density reduction.

$$P_v = 1 - 1.0287\sqrt{1 + \frac{2Q}{v_a^2}\left[Lsin\theta - \frac{\lambda v^2 L \times (vB^2 + Q)}{4QBg}\right]} + \frac{0.244}{v_a}\# \quad (18)$$

$$L = (N-1)D_y\# \quad (19)$$

$$\lambda = \frac{1}{(1-f_v)}\left[\frac{8n_0^2 g}{R^{\frac{1}{3}}} + \frac{4C_D \Sigma_{i=k}^{N} A_i}{\chi L}\right]\# \quad (20)$$

$$f_v - \frac{\sum_{i=1}^{M} T_{vi}}{AL}\# \quad (21)$$

$$R = \frac{A}{\chi} = \frac{(B - md)h}{2h(m+1) + B - md}\# \quad (22)$$

$$m = \left[\frac{B}{D_x}\right] + 1\# \quad (23)$$

$$M = N\left[\frac{B}{D_x}\right] + \frac{N}{2}\# \quad (24)$$

N is an even number, and B/D_x is not an integer.

$$M = N\left(\left[\frac{B}{D_x}\right] - 1\right) + \frac{N}{2}\# \quad (25)$$

N is an even number, and B/D_x is an integer.

$$M = N\left[\frac{B}{D_x}\right] + \frac{N+1}{2}\# \quad (26)$$

N is an odd number, and B/D_x is not an integer.

$$M = N\left(\left[\frac{B}{D_x}\right] - 1\right) + \frac{N+1}{2}\# \quad (27)$$

N is an odd number, and B/D_x is not an integer.

where P_v is the flow velocity reduction rate, v_a is the flow velocity before the filter strip, v_b is the flow velocity after the filter strip, D_x is the stem spacing, D_y is the row spacing, N is the number of rows, L is the length of the filter strip, B is the width of the valley, θ is the slope of the gully bed, λ is the friction coefficient, v is the average flow velocity ($v = v_a + v_b$), Q is the flow rate, and f_v is the submerged volume ratio of the trees in the debris flow, n_0 is the Manning roughness coefficient of the nonfiltered zone (i.e., the original gully bed roughness), R is the hydraulic radius, C_D is the flow resistance coefficient around the vegetation, which is generally related to the shape of the vegetation and the Reynolds number of the debris flow R_e, A_i is the projected cross-sectional area of a row of trees orthogonal to the flow direction, χ is the wetted perimeter, A is the flow area, T_{vi} is the submerged volume of each tree in the debris flow and is related to the plant species and surface morphological characteristics, M is the total number of plants in the filter strip, m is the number of trees in each row, d is the diameter of the trunks of the trees, and h is the submerged mud depth of the trees.

The flow velocity reduction Eqs. (17) and (18) for dilute and viscous debris flows, respectively, were verified, and the results are as follows.

The points in the scatterplot (Fig. 18) are distributed close to a straight line (y = x), indicating that the calculated values obtained using the flow velocity reduction Eqs. (17) and (18) for the dilute and viscous debris flows, respectively, were equal to the values measured in the experiment. This result demonstrates that utilizing these two equations

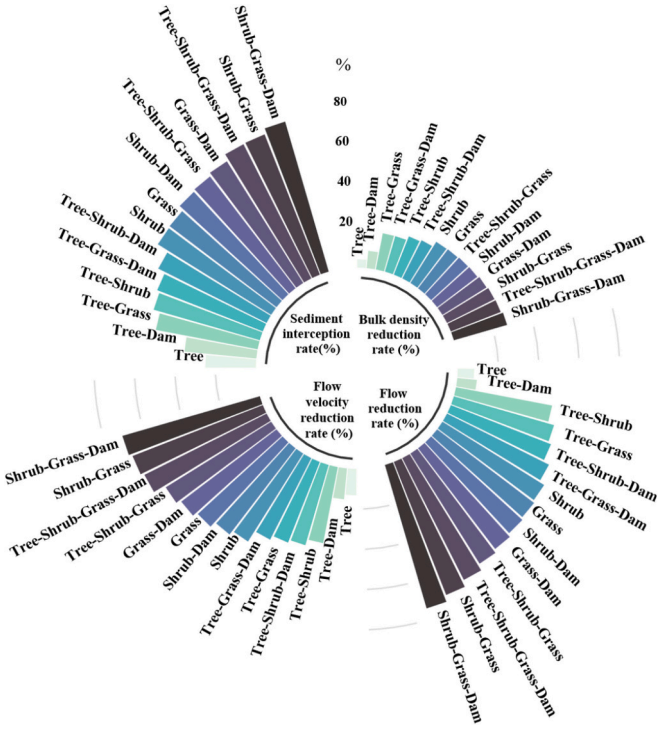

Fig. 16. Reduction in the movement of dilute debris flows using different combined models.

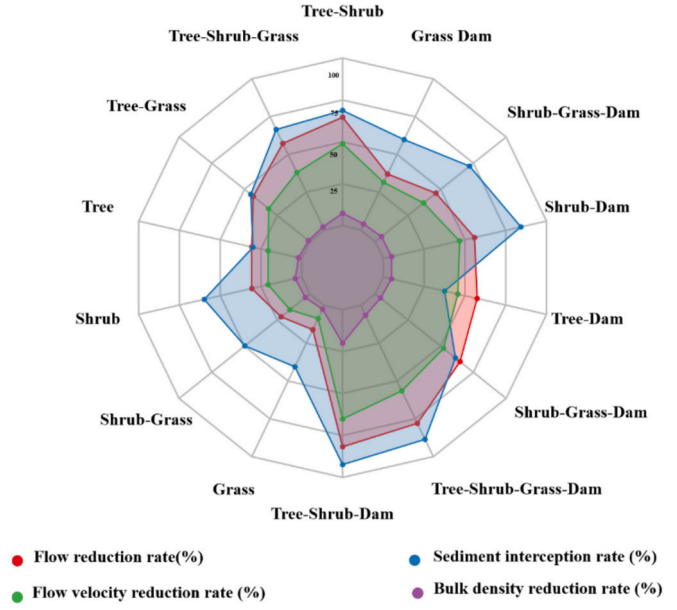

Fig. 17. Reduction rates on the movement of viscous debris flows using different combined models.

with the tree filter strips is an objective and reliable approach that can be applied in future projects.

The flow velocity equation used after the tree filter strip considers the vegetation arrangement (stem spacing, row spacing, number of rows, and so on), morphological characteristics of the vegetation, slope of the gully bed, debris flow characteristics (flow velocity and flow rate), and other influencing factors. When the debris flow characteristics, gully bed slope, and vegetation form are known, the flow velocity equation after the tree filter strip can be used to calculate the flow velocity after the filter strip v_b under different arrangements. Since the tree filter strip has a limited reduction on the specific weight of debris flows for both viscous and dilute debris flows, $\gamma_a = \gamma_b$; therefore, γ_a and γ_b cancel each other out in the formula, and the final formula for the flow velocity after the tree filter strip does not include the term γ, the specific weight of the debris flow. However, even if the specific weight of the debris flow γ is not included, the effect of the specific weight of the debris flow on the flow velocity after the tree filter strip, v_b, remains. When debris flows with different specific weights pass through the filter strip, the flow velocity before the strip v_a, mud depth h, and hydraulic radius R in the strip may differ. As a result, the specific weight of the debris flow affects the flow velocity after the strip v_b. To assess the flow velocity before strip v_a, further studies of the specific functional relationships between the specific weight of the debris flow, the mud depth h, and the hydraulic radius (R) are needed.

4.2. Comparison of the optimized eco-geotechnical measures (for dilute and viscous flows)

The principles of eco-geotechnical cooperative disaster mitigation aim for a low-input economy, a long-term mitigation efficacy, environmental friendliness, and a convenient application. Cooperative disaster mitigation is characterized by a division of labor in terms of function and complementary approaches over time. Specifically, upstream geotechnical engineering (comb-toothed dams) is functionally used to intercept boulders and glacial erratics and reduce the flow energy and destructive power of debris flows. By comparison, downstream vegetation filter strips are used to intercept debris, gravel, and sand; thus, sediment interception is accomplished using layers of filtration. Temporally, the implementation of geotechnical engineering projects in upstream areas provides immediate interception and protection as well as time for the growth of vegetation downstream, thus creating an advantageous environment for plant growth. After 5–10 years, vegetation grows and performs its functions such as intercepting debris flows, retaining water in the root system, and fixing soil. These functions improve the local microclimate and conditions for the initiation of debris flows, intercept debris flows when they are initiated, and lessen the pressure on geotechnical engineering for disaster mitigation. These two measures complement each other and ultimately achieve effective disaster mitigation.

This study focuses on the immediate interception rates of various combinations of these two measures and their resulting effects on disaster mitigation. According to the experimental results, the interception rates of the different models varied for different types of debris flows (dilute and viscous). For dilute debris flows, the shrub-grass (dam)

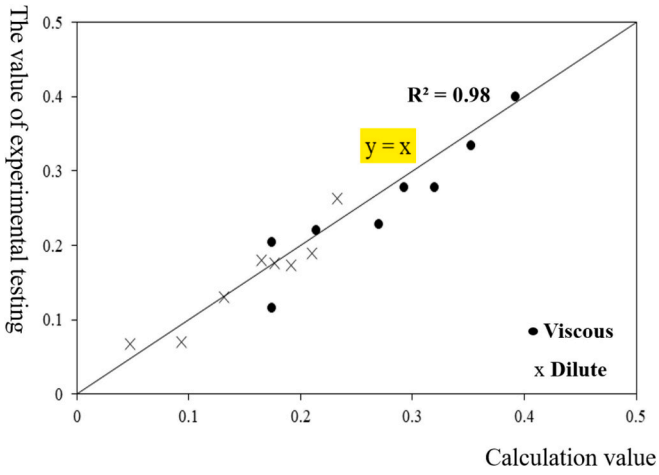

Fig. 18. Comparison of the calculated and measured values of the velocity reduction rate.

model had the strongest interception performance, and for viscous debris flows, the tree-shrub (dam) model was the most effective (Fig. 19). This difference mainly occurred due to variances in the energy reduction and material interception of viscous and dilute debris flows by the comb-toothed dam. As viscous debris flows have a high proportion of solid matter and a high fluid cohesion, they often move as a whole. Therefore, the comb-toothed dam had a pronounced interception rate for debris flows. Moreover, when a viscous debris flow passed through a dam gap, the internal drag force of the fluid hindered the movement of the viscous debris flow due to its integrity. The material and kinetic energy of the viscous debris flow passing through the first gradient of the comb-toothed dam were reduced. When the debris flow reached the vegetation, the stiffness of the trees allowed them to function similarly to a comb-tooth dam. In addition, shrubs increased the roughness of the surface, causing the tree-shrub (dam) model to have a higher performance than the other cooperative models for intercepting viscous debris flows. The proportion of solid matter in the dilute debris flows was relatively low. In dilute debris flows, water and rocks move separately. Therefore, comb-toothed dams mainly block coarse materials while allowing fine materials to pass through. When the debris flow reached the vegetation, the stem and row spacings of the shrubs were suitable for intercepting solid materials. Even when the flow rate increased, the increase in surface roughness substantially affected the movement of the dilute debris flow. Although trees are stiff and can block large materials, their spacing affects their interactions with these materials, and the overall interception efficacy is weaker than that caused by roughness. Therefore, the shrub-grass (dam) model was optimal for dilute debris flows.

4.3. A comparison with other related cooperative models

Debris flow prevention and control are fundamental and ongoing endeavors. Previous researchers have explored various measures, evolving from simplistic interception methods in traditional geotechnical engineering to current strategies that incorporate both interception and diversion measures. Specific measures have transitioned from solid gravity dams to parameter optimization and performance studies of permeable sediment trapping dams. The comb-toothed dam used in this study is inspired by the research findings of Sun et al. (2020) and others (Wang et al., 2020), reflecting the economic and practical aspects of disaster reduction. However, relying solely on geotechnical measures represents a passive approach to disaster reduction. The development of the concept of nature-based solutions has increased the emphasis on ecologically friendly, collaborative disaster-reduction methods, particularly eco-geotechnical collaborative measures. These measures not only achieve immediate interception of debris flows (passive disaster reduction), but also utilize vegetation to improve local site conditions through soil and water conservation (active disaster reduction), thereby achieving long-term effectiveness in debris flow prevention and control.

Although research on the collaborative disaster reduction mode and mechanism of eco-geotechnical cooperation is still in its infancy, several models have emerged. Ding et al. (2024) evaluated the collaborative mechanism between roots and piles for slope protection, but this model is applicable to the slope body rather than the valley-type debris flows, as proposed in this study. To prevent and control debris flows in the channel, Cui et al. (2023b) proposed an embedded collaborative model of check dams and vegetation, similar to the collaborative model proposed in this study (Fig. 20). This design focuses on interception and diversion to provide timely and immediate disaster prevention, while allowing space and time for vegetation to grow. As vegetation matures, it reduces damage to geotechnical measures, thereby consolidating the role of water retention and soil stabilization. However, Cui's model uses only shrubs and herbaceous plants. Compared with the segmented trees-shrubs-grasses model proposed in this study, its interception effect on debris flows is relatively small, and it is not conducive to the formation of ecological communities. Notably, this embedded cooperative model mainly aims to reduce the scouring and erosion of the dam body by perennial or hyper-concentration flow. Although researchers have also established formulas for calculating flow velocity under the influence of vegetation coverage, roughness, flow rate, and slope, the vegetation coverage considered in these formulas is primarily herbaceous.

Lyu et al. (2022) further considered the vegetation coverage of trees-shrubs-grasses and established an eco-geotechnical collaborative energy dissipation calculation model. However, their consideration of vegetation coverage remains relatively general, lacking specific parameters for the arrangement of vegetation rows and stem spacing, which limits

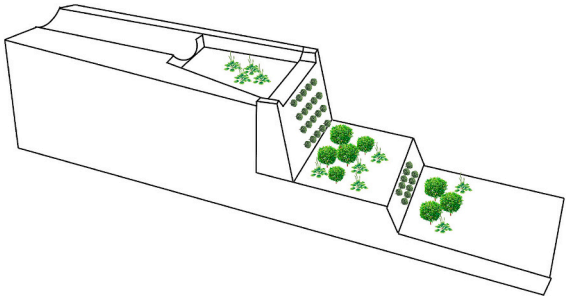

Fig. 20. An embedded collaborative model of check dams and vegetation.

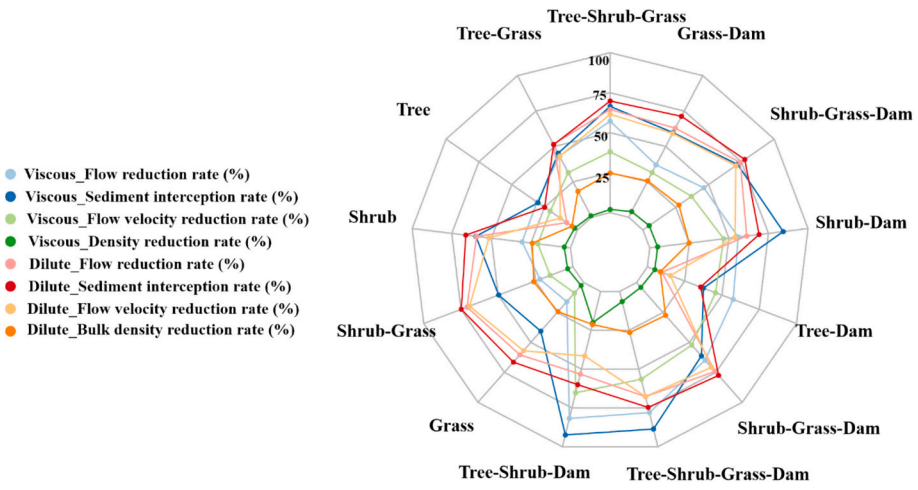

Fig. 19. Comparison of mitigation efficacies among all combination patterns.

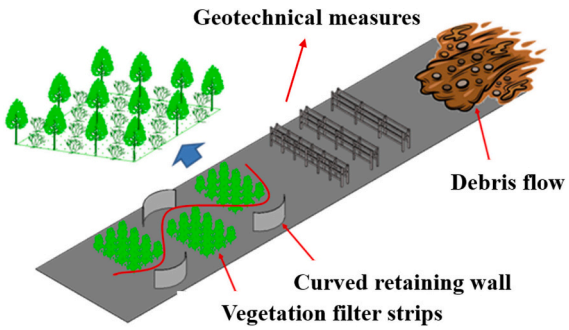

Fig. 21. A new cooperative model incorporating interception and drainage.

practical application. This study addresses that gap by establishing precise row and stem spacing parameters for vegetation. However, the derivation of the energy reduction relationship has not been covered. Subsequent to this study, the effects of different combination modes with different vegetation row and stem spacing on energy dissipation will be explored. Indeed, the current research on eco-geotechnical collaborative models and mechanisms must consider more disaster scenarios and factors involved and conduct deeper investigations into specific disaster mitigation benefits (sediment interception and energy reduction).

4.4. Limitations and future prospects

Geotechnical and ecological engineering measures influence disaster prevention to a certain extent; however, there are several problems with these approaches. Geotechnical engineering measures require a large amount of construction, are expensive, and have a considerable impact on the environment. The primary engineering materials used, such as steel and concrete, are incompatible with the natural environment. The prevention and control abilities of ecological engineering measures are limited, and a long period is required for vegetation to mature and influence soil and water conservation. Models that combine geotechnical and ecological engineering measures provide more comprehensive control. In this study, a whole-area segmented planting scheme was used. Although this approach is beneficial for preventing the occurrence of debris flows to a certain extent and has a better interception rate for low-frequency and small-scale debris flows, it is prone to causing the accumulation of debris flows in the future, posing greater potential harm. Moreover, the site conditions and species of trees, shrubs, and herbs used in segmented planting are prone to burial by large-scale debris flows, thus reducing control and limiting the application range of the proposed technology. Moreover, individually planted trees, shrubs, and herbaceous strips are not conducive to the formation of plant communities with a variety of vegetation types, leading to poor ecological restoration and reducing the overall ability of the vegetation to contribute to disaster prevention.

In future research, the design of eco-geotechnical measures should further consider the extent to which vegetation filter strips contribute to ecological restoration and the prevention of debris flows, as such measures can effectively block flows and reduce the potential for damage. To address the shortcomings of existing technologies, future eco-geotechnical measures should adhere to a cooperative engineering structure that considers both the containment of debris flows and the restoration of the ecological environment (Fig. 21). Furthermore, the staggered arrangement of vegetation should be used to create an "S"-shaped channel between structures. This newly proposed cooperative model ensures the smooth outflow of some of the debris flow; additionally, this pattern prevents the emergence of new threats from blockages formed by the siltation of the debris flow in the upstream and middle sections because the block is complete and strong. When there is a bend in a channel, debris flows can reach large heights, causing some of their kinetic energy of the debris flow to be converted into potential energy. In such instances, some of the kinetic energy is converted into internal energy and consumed because the incoming debris flow is affected by the convex bank of the bend, which causes the flows to collide. The concave and convex banks of bends in areas with vegetation decelerate debris flows.

5. Conclusions

Ecological and geotechnical engineering are two important measures for preventing debris flow disasters. Combining ecological and geotechnical engineering to control debris flow disasters is an important direction for multidisciplinary development in the field of debris flow prevention and is a manifestation of the concept of nature-based solutions for disaster prevention and control. In this study, vegetation filter strips composed of trees, shrubs, and grasses were used as ecological engineering measures and a comb-toothed dam was used as a geotechnical engineering measure. The effects of different arrangements (stem spacing and row spacing) of vegetation filter strips on debris-flow movement were investigated through field investigations and indoor flume simulation tests, and the effects of different combinations of these strips and comb-toothed dams on debris flow interception rates were analyzed. An optimized eco-geotechnical model consisting of a vegetation filter strip and a comb-toothed dam was constructed. And the sediment retention rate can reach up to 92 %, and energy reduction can reach up to 42 %. The relationships among the debris flow velocity, flow rate reduction, vegetation arrangement parameters (stem and row spacing), morphological characteristics of vegetation, slope, and roughness were determined to provide a scientific basis for analyzing the interception and movement characteristics of the combined models. This research represents a preliminary exploration of eco-geotechnical measures that currently help impede the movement of low-frequency and small-scale debris flows. Moreover, our study promotes the optimization and construction of local ecological environments to an extent. However, the prevention and control of high-frequency and large-scale debris flows are complex, therefore, additional combination models should be developed in future research.

CRediT authorship contribution statement

Songtang He: Writing – review & editing, Writing – original draft, Supervision, Methodology, Funding acquisition, Formal analysis, Data curation, Conceptualization. **Wenle Chen:** Software, Methodology, Investigation, Formal analysis, Conceptualization. **Xiaoqing Chen:** Writing – review & editing, Supervision, Project administration, Conceptualization. **Daojie Wang:** Writing – review & editing, Supervision, Conceptualization. **Yong Li:** Writing – review & editing, Supervision. **Zengli Pei:** Methodology, Investigation. **Peng Zhao:** Methodology, Investigation. **Yuchao Qi:** Methodology, Investigation.

Declaration of competing interest

The authors declare that they have no known competing financial interests or personal relationships that could have appeared to influence the work reported in this paper.

Acknowledgments

This work was financially supported by the National Key Research and Development Program of China (2024YFC3012702; 2024YFF1307801; 2024YFF1307800), the Youth Innovation Promotion Association of the Chinese Academy of Sciences (Grant No. 2023389), the National Natural Science Foundation of China (Grant No. 42201094; Grant No. 42371014), China Scholarship Council (CSC) for Academic Visiting (202404910203), and Science and Technology Research Program of the Institute of Mountain Hazards and Environment, Chinese

Academy of Sciences. We also would like to thank the Dongchuan Debris Flow Observation and Research Station (DDFORS, http://nsl.imde.ac.cn/en/), Chinese Academy of Sciences, which provides the field observation data and experimental site.

Data availability

Data will be made available on request.

References

Anderson, C.C., Renaud, F.G., 2021. A review of public acceptance of nature-based solutions: The 'why', 'when', and 'how' of success for disaster risk reduction measures. Ambio 50 (8), 1552–1573. https://doi.org/10.1007/s13280-021-01502-4.

Arnone, E., Caracciolo, D., Noto, L.V., Preti, F., Bras, R.L., 2016. Modeling the hydrological and mechanical effect of roots on shallow landslides. Water Resour. Res. 52 (11), 8590–8612. https://doi.org/10.1002/2015wr018227.

Booth, A.M., Sifford, C., Vascik, B., Siebert, C., Buma, B., 2020. Large wood inhibits debris flow runout in forested Southeast Alaska. Earth Surf. Process. Landf. 45 (7), 1555–1568. https://doi.org/10.1002/esp.4830.

Borja, P., Molina, A., Govers, G., Vanacker, V., 2018. Check dams and afforestation reducing sediment mobilization in active gully systems in the Andean mountains. Catena 165, 42–53. https://doi.org/10.1016/j.catena.2018.01.013.

Cerrillo, G.T., Rodríguez, J.L., Spain, N.M., 2016. Monitoring of erosion preventive structures based on eco - engineering approaches: The case of the mixed check dams of masonry and forest residues. J. Eng. Sci. Tech. Rev. 9, 103–107. https://api.semanticscholar.org/CorpusID:116426794.

Chirico, G.B., Borga, M., Tarolli, P., Rigon, R., Preti, F., 2013. Role of vegetation on slope stability under transient unsaturated conditions. Procedia Environ. Sci. 19, 932–941. https://doi.org/10.1016/j.proenv.2013.06.103.

Cui, P., Lin, Y., 2013. Debris-flow treatment: the integration of botanical and geotechnical methods. J. Resources Ecol. 4 (2), 97–104. https://doi.org/10.5814/j.issn.1674-764x.2013.02.001.

Cui, P., Peng, J., Shi, P., Tang, H., Ouyang, C., Zou, Q., et al., 2021. Scientific challenges of research on natural hazards and disaster risk. Geogr. Sustain. 2 (3), 216–223. https://doi.org/10.1016/j.geosus.2021.09.001.

Cui, W.R., Chen, J.G., Chen, X.Q., Tang, J.B., Jin, K., 2023a. Debris flow characteristics of the compound channels with vegetated floodplains. Sci. Total Environ. 868, 161586. https://doi.org/10.1016/j.scitotenv.2023.161586.

Cui, W.R., Chen, X.Q., Chen, J.G., Zhao, W.Y., 2023b. Protection method for the dam body and foundation of check dam. CN202010990371.4. China, 2023-07-18. https://cprs.patentstar.com.cn/.

Ding, H., Xue, L., Shang, J., et al., 2024. Study on synergistic action of tap-like arbor root system and anti-slide piles by physical model experiment of landslides. Landslides 21, 1707–1717. https://doi.org/10.1007/s10346-024-02248-2.

Guthrie, R.H., Hockin, A., Colquhoun, L., Nagy, T., Evans, S.G., Ayles, C., 2010. An examination of controls on debris flow mobility: evidence from coastal British Columbia. Geomorphology 114 (4), 601–613. https://doi.org/10.1016/j.geomorph.2009.09.021.

He, S.T., Chen, W.L., Wang, D.J., Chen, X.Q., Qi, Y.C., Zhao, P., Li, Y., Lin, L.Y., Jamali, Ali Akbar, 2023. Experimental investigation of the effects of shrub filter strips on debris flow trapping and interception. Int. J. Sedim. Res. 38 (2), 265–278. https://doi.org/10.1016/j.ijsrc.2022.09.005.

Heller, V., 2011. Scale effects in physical hydraulic engineering models. J. Hydraul. Res. 49 (3), 293–306. https://doi.org/10.1080/00221686.2011.578914.

Huai, W.-X., Li, S., Katul, G.G., Liu, M.-Y., Yang, Z.-H., 2021. Flow dynamics and sediment transport in vegetated rivers: a review. J. Hydrodyn. 33 (3), 400–420. https://doi.org/10.1007/s42241-021-0043-7.

Huang, Y., Zhang, B., 2022. Challenges and perspectives in designing engineering structures against debris-flow disaster. Eur. J. Environ. Civ. Eng, 26 (10), 4476–4497. https://doi.org/10.1080/19648189.2020.1854126.

Jin, K., Chen, J., Chen, X., Zhao, W., Si, G., Gong, X., 2021. Impact failure models and application condition of trees in debris-flow hazard mitigation. J. Mt. Sci. 18, 1874–1885. https://doi.org/10.1007/S11629-020-6510-8.

Kinol, A.D., Arango-Quiroga, J., Kuhl, L., 2023. Opportunities for nature-based solutions to contribute to climate-resilient development pathways. Curr. Opin. Environ. Sustain. 62, 101297. https://doi.org/10.1016/j.cosust.2023.101297.

Kwan, J.S.H., Koo, R.C.H., Ng, C.W.W., 2015. Landslide mobility analysis for design of multiple debris-resisting barriers. Can. Geotech. J. 52 (9), 1345–1359. https://doi.org/10.1139/cgj-2014-0152.

Lobovský, L., Botia-Vera, E., Castellana, F., Mas-Soler, J., Souto-Iglesias, A., 2014. Experimental investigation of dynamic pressure loads during dam break. J. Fluids Struct. 48, 407–434. https://doi.org/10.1016/j.jfluidstructs.2014.03.009.

Lyu, L.Q., Xu, M.Z., Zhou, G.Y., et al., 2022. Quantitative evaluation of eco-geotechnical measures for debris flow mitigation by improved vegetation-erosion model. J. Mt. Sci. 19 (7). https://doi.org/10.1007/s11629-021-7285-2.

Marchesini, I., Althuwaynee, O., Santangelo, M., et al., 2024. National-scale assessment of railways exposure to rapid flow-like landslides. Eng. Geol. 332, 107474. https://doi.org/10.1016/j.enggeo.2024.107474.

Mcardell, B.W., Bartelt, P., Kowalski, J., 2007. Field observations of basal forces and fluid pore pressure in a debris flow. Geophys. Res. Lett. 340 (7). https://doi.org/10.1029/2006GL029183.

Ng, C.W.W., Choi, C.E., Liu, L.H.D., Wang, Y., Song, D., Yang, N., 2017. Influence of particle size on the mechanism of dry granular run-up on a rigid barrier. Géotechn. Lett. 7 (1), 79–89. https://doi.org/10.1680/jgele.16.00159.

Pudasaini, S.P., Mergili, M., 2019. A multi-phase mass flow model. J. Geophys. Res. Earth 124, 2920–2942. https://doi.org/10.1029/2019JF005204.

Rey, F., Bifulco, C., Bischetti, G.B., et al., 2019. Soil and water bioengineering: Practice and research needs for reconciling natural hazard control and ecological restoration. Sci. Total Environ. 648, 1210–1218. https://doi.org/10.1016/j.scitotenv.2018.08.217.

Riaz, M., Basharat, M., Ahmed, K., et al., 2024. Failure mechanism of a massive fault–controlled rainfall–triggered landslide in northern Pakistan. Landslides 21, 2741–2767. https://doi.org/10.1007/s10346-024-02342-5.

Sarkar, A., Singh, V., Parida, S., 2024. Geomorphic assessment of sediment storage potential and mobilisation on the hillslopes of a mountain catchment: an example from Pranmati catchment, NW Himalaya. Geomorphology 463, 109351. https://doi.org/10.1016/j.geomorph.2024.109351.

Song, D., Chen, X., Sadeghi, H., Zhong, W., Hu, H., Liu, W., 2023. Impact behavior of dense debris flows regulated by pore-pressure feedback. J. Geophys. Res. Earth 128, e2023JF007074. https://doi.org/10.1029/2023JF007074.

Song, D., Chen, X., Zhou, G., Lu, X., Cheng, G., Chen, Q., 2021. Impact dynamics of debris flow against rigid obstacle in laboratory experiments. Eng. Geol. 291, 106211. https://doi.org/10.1016/j.enggeo.2021.106211.

Stokes, A., Douglas, G.B., Fourcaud, T., Giadrossich, F., Gillies, C., Hubble, T., et al., 2014. Ecological mitigation of hillslope instability: ten key issues facing researchers and practitioners. Plant Soil 377 (1–2), 1–23. https://doi.org/10.1007/s11104-014-2044-6.

Sun, H., You, Y., Liu, J., Zhang, G., Feng, T., Wang, D., 2020. Experimental study on discharge process regulation to debris flow with open-type check dams. Landslides 18 (3), 967–978. https://doi.org/10.1007/s10346-020-01535-y.

Tjalling, de H., Braat, L., Leuven, J., Lokhorst, I., Kleinhans, M., 2015. Effects of debris flow com-position on runout, depositional mechanisms, and deposit morphology in laboratory experiments. J. Geo-phys. Res. Earth Surf. 120, 1949–1972. https://doi.org/10.1002/2015JF003525.

Vannoppen, W., De Baets, S., Keeble, J., Dong, Y., Poesen, J., 2017. How do root and soil characteristics affect the erosion-reducing potential of plant species? Ecol. Eng. 109, 186–195. https://doi.org/10.1016/j.ecoleng.2017.08.001.

Wahren, A., Schwärzel, K., Feger, K.H., 2012. Potentials and limitations of natural flood retention by forested land in headwater catchments: evidence from experimental and model studies. J. Flood Risk Manag. 5 (4), 321–335. https://doi.org/10.1111/j.1753-318x.2012.01152.x.

Wang, X., Ma, C., Wang, Y., Wang, Y., Li, T., Dai, Z., Li, M., 2020. Effect of root architecture on rainfall threshold for slope stability: Variabilities in saturated hydraulic conductivity and strength of root-soil composite. Landslides 17 (8), 1965–1977. https://doi.org/10.1007/s10346-020-01422-6.

Wu, X., Lü, Y., Zhang, J., Lu, N., Jiang, W., Fu, B., 2023. Adapting ecosystem restoration for sustainable development in a changing world. Innovation 4 (1), 100375. https://doi.org/10.1016/j.xinn.2023.100375.

Xu, Y., Luo, L., Guo, W., Jin, Z., Tian, P., Wang, W., 2024. Revegetation changes main erosion type on the gully–slope on the Chinese loess plateau under extreme rainfall: reducing gully erosion and promoting shallow landslides. Water Resour. Res. 60 (3), e2023WR036307. https://doi.org/10.1029/2023wr036307.

Zhao, C., Gao, J., Zhang, M., Wang, F., Zhang, T., 2016. Sediment deposition and overland flow hydraulics in simulated vegetative filter strips under varying vegetation covers. Hydrol. Process 30, 163–175. https://doi.org/10.1002/hyp.10556.

Zou, Y.H., Chen, X.Q., 2015. Effectiveness and efficiency of slot-check dam system on debris flow control. Nat. Hazards Earth Syst. Sci. Discus. 3 (9), 5777–5804. https://doi.org/10.5194/nhessd-3-5777-2015.